Sensors & Actuators: B. Chemical 298 (2019) 126878

Contents lists available at ScienceDirect

Sensors and Actuators B: Chemical

journal homepage: www.elsevier.com/locate/snb

Highly sensitive H_2O_2 sensor based on poly(azure A)-platinum nanoparticles deposited on activated screen printed carbon electrodes

Rebeca Jiménez-Pérez[a], José González-Rodríguez[b], María-Isabel González-Sánchez[a], Beatriz Gómez-Monedero[a], Edelmira Valero[a,*]

[a] Department of Physical Chemistry, Higher Technical School of Industrial Engineering, University of Castilla-La Mancha, Campus Universitario s/n, 02071, Albacete, Spain
[b] School of Chemistry, College of Science, University of Lincoln, Brayford Pool, Lincoln, LN6 7TS, UK

ARTICLE INFO

Keywords:
Electrochemical sensor
Hydrogen peroxide
Poly(azure A)
Platinum nanoparticles
Modified electrodes
Screen-printed carbon electrodes

ABSTRACT

The sensitive determination of hydrogen peroxide has broad analytical applications. In this work, a novel non-enzymatic hydrogen peroxide sensor based on Pt nanoparticles (PtNPs) electrochemically deposited on previously modified and activated screen-printed carbon electrodes (aSPCEs) was constructed. The pretreatment consisted of subjecting the electrodes to a surface activation treatment with hydrogen peroxide followed by the electrodeposition of poly(azure A) films (PAA) in a sodium dodecyl sulfate micellar aqueous solution. The PtNPs/PAA/aSPCEs were characterized by scanning electron microscope, X-Ray photoelectron spectrometry, linear scan voltammetry and electrochemical impedance spectroscopy. Linear sweep voltammograms showed that the oxidation peak potential of H_2O_2 shifts from ˜1 V at SPCEs to ˜0.1 V at PtNPs/PAA/aSPCEs. The fabricated electrodes showed excellent electrocatalytic activity towards H_2O_2 oxidation, making its detection possible at 0.1 V. The detection limit was 51.6 nM, which is significantly lower than other modified electrodes found in the literature, and the linear range ranging from 0 to 300 μM. The proposed electrode was successfully applied to the determination of H_2O_2 in real samples in different areas. Additional experiments against common interfering agents (ascorbic acid, dehydroascorbic acid, glucose, salicylic acid, among other compounds) showed no increase in the current signal and only in the case of ascorbic acid a small interference, not greater than 10% is observed, which indicates high specificity of the sensor. These electrodes open up alternative avenues for the development of highly sensitive, robust and low cost electrochemical H_2O_2 sensors for field tests.

1. Introduction

Hydrogen peroxide (H_2O_2) has a wide range of applications in different fields such as clinic, chemical engineering, cleaning, textile, pharmaceuticals, food industry and environmental sciences [1–3]. It is also an important compound in life processes acting as a reaction intermediate. Therefore, a simple, cheap, quick, sensitive and precise determination of H_2O_2 is not only of interest but also necessary. To date, various measurement methods based on titrimetry, spectrophotometry, fluorescence, chemiluminescence, resonance light scattering [4,5] have been used to detect H_2O_2. However, these methods cannot be applied to real-time measurement of H_2O_2 and many of them are expensive, time-consuming and complex. Electrochemical methods have many practical advantages such as high sensitivity and accuracy, selectivity, short response time, portability, low cost, ease of operation and the ability to offer reliable responses in real time, even in complex biological systems [6]. In recent years, the electrocatalytic determination of H_2O_2 attending to its reduction or oxidation and using different types of modified electrodes [7,8], has been widely studied. Among them, the enzyme-based electrochemical biosensors offer the advantage of high selectivity and sensitivity [9]. However, their application is limited by the relatively high cost of enzymes, tedious immobilization procedures, low reproducibility and environmental instability [10]. Therefore, further development of non-enzymatic electrodes based on various nanomaterials, with excellent electrocatalytic properties, high surface-to-volume ratio, stability and low cost, is strongly desirable [11].

The selection of the electrode material is very important in electrochemical studies since the type of substrate and its modification generally affect the sensitivity, selectivity, stability and the cost of the developed electrochemical sensors. Screen-printed electrodes (SPEs) are being increasingly used in practically all fields of Chemistry [12,13]

* Corresponding author.
E-mail addresses: Rebeca.Jimenez@uclm.es (R. Jiménez-Pérez), jgonzalezrodriguez@lincoln.ac.uk, MIsabel.Gonzalez@uclm.es (M.-I. González-Sánchez), Beatriz.Gomez@uclm.es (B. Gómez-Monedero), Edelmira.valero@uclm.es (E. Valero).

https://doi.org/10.1016/j.snb.2019.126878
Received 13 March 2019; Received in revised form 3 July 2019; Accepted 25 July 2019
Available online 26 July 2019
0925-4005/

as they offer a number of advantages over conventional electrodes. One of the best known advantages of such electrodes is the easy modification to develop different sensing surfaces. Furthermore, pre-treatments can be performed in order to enhance electro-transfer properties and improve sensitivity to analytes of interest [14,15].

Nowadays, advances in new materials for the modification of electrodes have had a notable impact on electroanalytical techniques. Recently, conducting polymers (CPs) and their nanocomposites have been widely used in preparing sensors to improve their performance characteristics [16]. CPs are considered to be useful matrices for the immobilization of catalytically active noble metal particles not only because of their porous structure and high surface area but also due to their relatively high electric conductivity [17]. Furthermore, the electrochemical properties of CPs make it possible to shuttle the electrons through polymer chains between the electrode and dispersed metal particles, where the electrocatalytic reaction occurs [18]. The electrosynthesis procedure of CPs is essential to obtain specific electrochemical and conducting properties [19,20]. Electropolymerization of azines and derivatives such as neutral red, azure A or methylene blue provides an important class of CPs with numerous applications as electrochemical sensors [21,22]. Among them, in this work we have focused our attention on poly(azure A) (PAA). The electropolymerization was performed in the presence of the surfactant sodium dodecyl sulfate (SDS) as doping agent in order to enhance conducting properties [23,24]. PAA(SDS) films showed better electrochemical and catalytic properties than others PAA synthesized with other different anions [19,22].

Platinum nanoparticle-modified electrodes are one of the most important materials used for the electrochemical detection of H_2O_2 because they show unique electronic and catalytic properties as well as good chemical stability, convenience of electron transfer and biocompatibility [25,26]. Additionally, PtNPs are shown to decrease the oxidation/reduction overvoltage in the determination of H_2O_2 [27], which is important to avoid interferences from other co-existing substances. Many studies related to electrochemical sensors based on metal nanoparticles have also mentioned that the metal loading, particle-size and stability have significant effects on the sensing performance [8,28,29].

The main objective of this work was to develop a convenient and sensitive electrochemical method for the determination of H_2O_2 taking advantage of the unique properties of CPs combined with the properties of PtNPs by using a previously activated SPCE. This first step allowed the easy *in situ* functionalization of the carbon ink with the introduction of new carbon-oxygen groups, which provides more surface anchoring groups on the electrode [15]. PAA was prepared on the activated electrode surface and PtNPs were electrogenerated on the polymer. By combining all these processes (activation of the surface, electrochemical polymerization and electrochemical generation of PtNPs) it has been possible to reduce H_2O_2 oxidation potential from ~1-0.7 V to 0.1 V (which will considerably minimize the effect of interfering species), as well as significantly improving sensitivity compared to other electrochemical sensors found in the literature. The proposed modified electrode has also been used as a sensor for H_2O_2 determination in real samples.

2. Materials and methods

2.1. Reagents

Ascorbate oxidase from Cucurbita sp. (156.60 units/mg solid), L-ascorbic acid (sodium salt), azure A (80%), chloroplatinic acid hexahydrate (≥99.9%), citric acid (trisodium salt), L-dehydroascorbic acid (DHA), D(+)-glucose, H_2O_2 (35%), D-mannitol, resveratrol, salicylic acid, sodium dodecyl sulfate (SDS 95%) and urea were purchased from Sigma-Aldrich. Reagents for the spectrophotometric measurement of H_2O_2 by the colorimetric xylenol orange method (ammonium iron (II) sulfate hexahydrate, D(-)-sorbitol and xylenol orange (disodium salt)) were also acquired from Sigma-Aldrich. KCl was obtained from Scharlau (Barcelona, Spain) and KNO_3 from Fluka. K_2HPO_4, KH_2PO_4 and $K_4Fe(CN)_6$ were sourced from Merck. H_2SO_4 and HCl were obtained from Panreac. The samples of antiseptic (3% hydrogen peroxide), liquid oxygen bleaches for colored (chemical composition declared: 5–15% oxygenated bleaching, < 5% anionic surfactants and non-ionic surfactants, perfume and preservatives (methylchloroisothiazolinone, methylisothiazolinone)) and white clothing (chemical composition declared: 5–15% oxygenated bleaching, < 5% anionic surfactants and non-ionic surfactants, optical whitening and perfume) and hair lightener (chemical composition declared: water, alcohol denat, *Chamomilla recutita* flower extract, hydrogen peroxide, parfum, phosphoric acid, amyl cinnamal, coumarin, linalool) were purchased from a local supermarket. Liquid oxygen solution for plants (11.9% hydrogen peroxide solution) was from Growth Technology.

Solutions were daily prepared with deionized water purified by a Milli-Q purification system (18.2 MΩ cm) (Millipore Corp, Bedford, MA, USA). The H_2O_2 stock solution was freshly prepared every day and its concentration was determined by measuring the absorbance at 240 nm (ε = 43.6 $M^{-1}\,cm^{-1}$) [30].

2.2. Apparatus

The SEM images were acquired using a FEI Quanta Inspect (Czech Republic) using FEI Software version 4.1.0.1910. The image processing software ImageJ [31] was used to obtain the particle size of PtNPs. The EDX imaging was acquired using a INCAx-act from Oxford Instruments (United Kingdom) and using INCA suite version 4.11 for data analysis. Electrochemical measurements were performed on an AUTOLAB potentiostat-galvanostat set-up (PGSTAT 204) controlled by the NOVA 2.0 software package for the total control of the experiments and data acquisition. The electrodes used were disposable screen-printed carbon electrodes (SPCEs) (DRP-110, DropSens), which consist of a carbon ink working electrode, a carbon counter electrode and a silver pseudo-reference electrode. Unless otherwise indicated, all potentials given in this paper are referred to the Ag-SPCE pseudo-reference electrode. Electrochemical impedance spectroscopy (EIS) was performed using a computer-controlled potentiostat AUTOLAB PGSTAT 128 N (Eco Chemie B.V) equipped with a frequency response analyzer (FRA) module. EIS was carried out at 0.14 V in 5 mM potassium ferrocyanide and 0.1 M KCl aqueous solution. Electrodes were polarized for 60 s. A sinusoidal small amplitude potential perturbation (5 mV *rms*) was subsequently superimposed between 65 kHz and 10 mHz, with five points per decade.

The X-ray photoelectronic spectroscopy (XPS) experiments were recorded by a K-Alpha Thermo Scientific spectrometer using Al-Kα (1486.6 eV) radiation, monochromatized by a twin crystal monochromator to yield a focused X-ray spot with a diameter of 400 μm mean radius. The alpha hemispherical analyzer was used as an electron energy analyzer that operates in the fixed analyzer transmission mode, with survey scan pass energy of 200 eV and 40 eV narrow scans. Processing of the XPS spectra was performed using the Avantage software, with energy values referenced to the C 1s peak of adventitious carbon located at 284.6 eV.

Spectrophotometric measurements were taken in a UV/Vis Perkin-Elmer Lambda 35 (PerkinElmer Instruments, Waltham, USA) spectrophotometer.

2.3. Preparation of modified electrodes

Firstly, electrodes were pretreated in agreement with the activation protocol recently reported by González-Sánchez et al. [15]. Briefly, 25 repetitive cyclic voltammetry scans were performed at 10 $mV{\cdot}s^{-1}$ between 1.0 and -0.7 V in 10 mM H_2O_2 (in 0.1 M PB, pH 7). Then the activated electrodes (aSPCEs) were rinsed with deionized water and

dried in air.

PAA films were electrogenerated on the surface of the working electrode of aSPCEs as described by Agrisuelas et al. [19]. The electrosynthesis solution consisted of an aqueous solution of 1 mg/mL azure A in 0.02 M SDS. Twenty voltammetric cycles were carried out between -0.25 and 1 V at 10 $mV{\cdot}s^{-1}$ (initial potential, E_i = 0.5 V). A platinum wire (CHI 115, CH instruments, Inc., USA) was used as the counter electrode during PAA electrosynthesis to keep the SPCE counter electrode integrity. After deposition, the modified electrodes (PAA/aSPCEs) were rinsed with abundant ethanol to remove the residual monomers adsorbed on PAA films, then cleaned with double-distilled water to eliminate residual ethanol and dried under nitrogen stream.

To obtain the platinized surface, a PAA/aSPCE was immersed into 5 mL of 0.8 mM platinum solution (H_2PtCl_6) containing 0.01 M KCl as supporting electrolyte. The pH of this solution was adjusted to 1.34 and after that, a constant potential of -0.4 V (*vs* Ag/AgCl external reference electrode) was applied for 900 s. The pseudo-reference electrode of the PAA/aSPCE was covered with paraffin film (Parafilm M®, USA) and an Ag/AgCl external reference electrode (CHI 111, CH instruments, Inc., USA) was used to avoid any possible alteration of the SPCE reference electrode. They were subsequently cleaned with double-distilled water.

The electroactive surface area of the electrodes was determined using the hydrogen adsorption/desorption voltammetric peaks of platinum electrode with a known charge density of 210 $\mu C{\cdot}cm^{-2}$ in 0.5 M H_2SO_4 [32]. A value of 0.35 ± 0.05 cm^2 was found for the modified electrodes herein prepared. These electrodes (PtNPs/PAA/aSPCEs) can be stored for several months and reutilized after electrochemical cleaning in PB 0.1 M pH 7, between -0.8 to 1.05 V and 0.1 $V{\cdot}s^{-1}$.

2.4. Hydrogen peroxide sensing

All the electrochemical measurements were carried out at a temperature of ˜25 °C. The amperometric technique was used to evaluate the sensor capabilities of the PtNPs/PAA/aSPCEs towards H_2O_2 and to compare them with non-modified SPCEs, aSPCEs and PAA/aSPCEs. To demonstrate the importance of the pretreatment performed in the electrode, the comparison was also made with an electrode platinized with the same method on a surface without any previous modification (PtNPs/SPCE). The polarization potential was fixed at 0.1 V *vs.* the Ag-SPCE pseudo-reference. Calibrations were performed by successive additions of H_2O_2 to attain final concentrations of 0.2, 0.4, 0.8, 2 and 10 μM to the background electrolyte (0.1 M PB pH 7) into the cell (5 mL initial volume) under magnetic stirring and by measuring the current intensity after stabilization.

Hydrogen peroxide concentration in the real samples was additionally measured by the conventional xylenol orange method at 550 nm following the instructions given by the supplier [33].

The experimental data were processed by the software package 'OriginPro 9.4'.

3. Results and discussion

3.1. Surface morphological characterization of PtNPs/PAA/aSPCEs. SEM and XPS

The surface morphology of the electrode through the different steps of the process: bare electrode (SPCE); activated SPCE (aSPCE); activated and polymerized electrode (PAA/aSPCE); and activated, polymerized and platinized electrode (PtNPs/PAA/aSPCE) was characterized using scanning electron microscopy (SEM) and the images are displayed in Fig. 1. As it can be seen in the SEM images, no significant changes were observed in the surface of the first three electrodes (SPCE, aSPCE and PAA/aSPCE, Figs. 1A, 1B and 1C, respectively). However, with respect to the fourth modified electrode (PtNPs/PAA/aSPCE, Fig. 1D), which is the selected working electrode, the differences are evident. From image 1D, it is possible to distinguish the spherical nanostructure of PtNPs with the particle size mainly distributed around 100 ± 10 nm decorating evenly the surface of the PAA/aSPCE. Although the nanoparticles do not have uniform size they are homogeneously distributed throughout the surface of the working electrode. In order to evaluate the changes presented after each modification and the existence of the elements, the EDX spectrum was also taken and is presented in Figs. S1 and S2 of Supplementary Material.

To further verify that each new modification of the electrode was successfully performed, the electrodes were characterized using XPS. First, a comparison between SPCE-aSPCE, and PAA/SPCE-PAA/aSPCE is summarized in Table 1. The electrochemical activation treatment introduced oxygenated functional groups, in agreement with [15] (5,51% in SPCE but 14.8% in aSPCE). The number of oxygen-containing functional groups on the surface of pretreated electrodes directly correlates with the rate of electron transfer for a particular redox system and also helps proton or electron exchanging. Consequently, reaction kinetics are affected in a positive way and the electrode becomes more sensitive towards the target analyte [34]. It is also important to highlight the role of the activation process in the polymer. The analysis of the N1 s showed that the loading amount of N on the surface of PAA/aSPCE (9.4%) was higher than that for PAA/SPCE (6.9%), which would point out that more polymer has been electrodeposited on aSPCEs, with the corresponding increase of the available surface for PtNPs deposition.

Fig. S3 shows the XPS survey spectrum of the PtNPs/PAA/aSPCE within the 0 to 1350 eV binding energy range, while the inset shows the XPS spectrum from 65 to 85 eV. The Pt $4f_{7/2}$ and $4f_{5/2}$ peaks are present at 71.08 and 74.40 eV, respectively, as shown from the inset. These binding energies values are the same as that of bulk Pt, indicating the formation of Pt in the zero valent state [35].

3.2. Electrochemistry of the modified and unmodified electrodes

The electrochemical interfacial properties of the different modified SPCEs at the electrode and electrolyte interface were investigated by electrochemical impedance spectroscopy (EIS) and cyclic voltammetry (CV). Fig. 2 shows the Nyquist plots of the (A) SPCE, (B) aSPCE, (C) PAA/aSPCE and (D) PtNPs/PAA/aSPCE in 0.1 M KNO_3 containing 5 mM $[Fe(CN)_6]^{4-}$, applying a constant DC potential of 0.14 V. The Nyquist plot of the EIS includes a semicircle at high frequencies which refers to the electron-transfer limiting process and a linear part at low frequencies related to the diffusion limiting process, fitting in all cases to a Randles type circuit [36]. The diameter of semicircular portion is equal to the charge transfer resistance (R_{ct}), which shows the kinetics of electron transfer of the redox probe at the electrode interface. The inset in Fig. 2A corresponds to the equivalent model circuit used to fit these data represented along with the respective values of R_{ct} and impedance (Z) measured at a frequency value of 0.1 Hz. As can be seen in the tabulated values of Fig. 2, R_{ct} dramatically decreased after each treatment of the electrode surface, obtaining the highest resistance value for the bare SPCE (1,982.80 Ω) and the lowest value for the PtNPs/PAA/aSPCE (436.43 Ω). Moreover, the impedance measurement at low frequencies (0.1 Hz) confirms that there is a decrease of the impedance in the mentioned modified electrodes in a parallel way to that observed for R_{ct}. These results explain the higher conductivity of the proposed sensor material.

In addition, the electron transfer behavior of the aforementioned electrodes was investigated by CV. The current response of the different modified electrodes in the absence and presence of 5 mM $[Fe(CN)_6]^{4-}$ was mathematically subtracted. The voltammograms obtained in this way (Fig. 3) were named background-subtracted cyclic voltammograms. The ΔEp values were calculated from the CV obtained, observing a decreasing difference between the anodic and cathodic peaks with each new modification of the electrode (ΔEp (SPCE) = 0.136 V; ΔEp (aSPCE) = 0.126 V; ΔEp (PAA/aSPCE) = 0.099 V; ΔEp (PtNPs/PAA/aSPCE) = 0.077 V). These results fit well with those previously

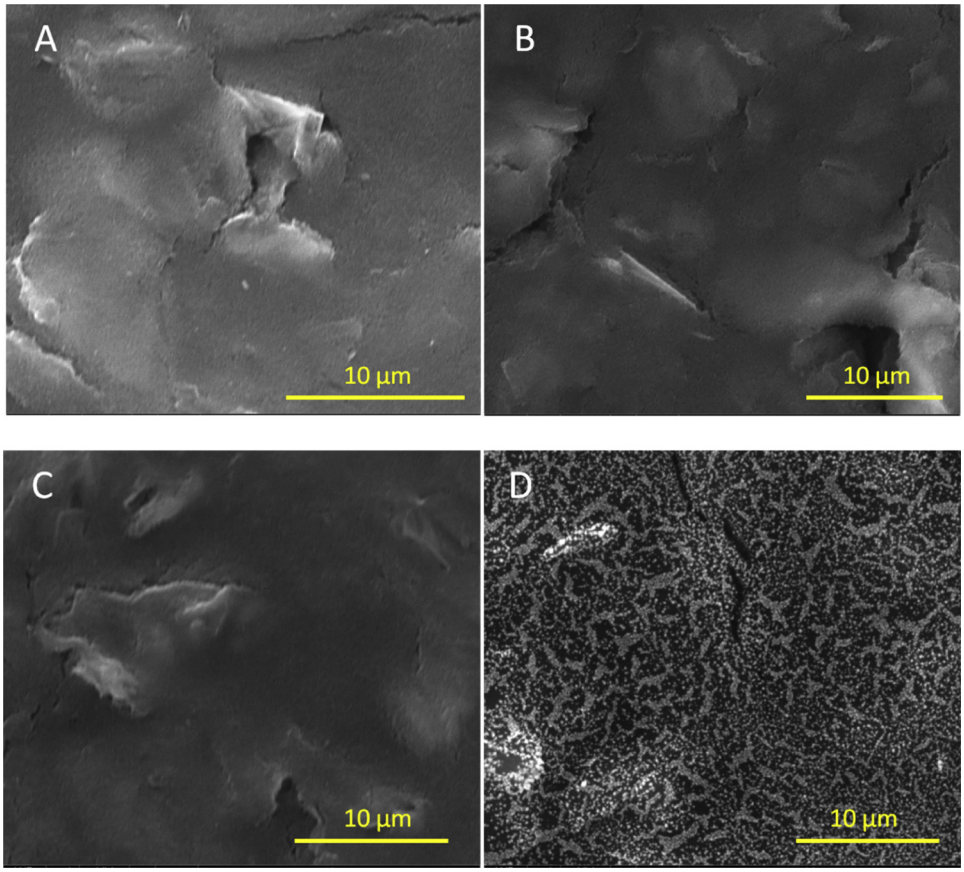

Fig. 1. SEM images of the different electrode modification steps: SPCE (A), aSPCE (B), PAA/aSPCE (C), PtNPs/PAA/aSPCE (D).

Table 1
The XPS results for the untreated SPCEs and electrodes subjected to activation and/or polymerization pretreatments.

	C1s at.%	O1s at.%	N1s at.%	Ref.
SPCE	94.35	5.51	–	[15]
aSPCE	93.68	14.8	–	
PAA/SPCE	79.58	13.52	6.9	This work
PAA/aSPCE	75.22	15.39	9.4	

obtained by EIS and suggest that PtNPs/PAA/aSPCEs are excellent electrode materials for the proposed sensor.

3.3. Electrochemical response of modified/unmodified SPCEs towards H_2O_2

The electrochemical behavior of H_2O_2 at the different electrocatalytic surfaces was assessed by linear sweep voltammetry (LSV). Fig. 4 shows the LSVs of the differently modified SPCEs in the absence (1a, 2a, 3a and 4a) and presence (1b, 2b, 3b and 4b) of 10 mM H_2O_2 in phosphate buffer (pH 7) solution at the scan rate of 50 mV/s. In all cases, and as a consequence of the successive modifications made to the conductive carbon ink, the oxidation peak of hydrogen peroxide was shifted towards lower potentials (the oxidation wave shifted from ˜1 V in SPCEs to ˜0.8 V in aSPCEs, ˜0.7 V in PAA/aSPCEs and ˜0.1 V in PtNPs/PAA/aSPCEs). This finding is very important in the development of amperometric (bio)sensors to minimize interference effects, background currents and noise which can be too high at overpotentials, adversely influencing the oxidation/reduction peak currents. Therefore in amperometry, it is always preferable to work at low oxidation potentials for the development of reliable (bio)sensors.

These results agree with those found in the literature. It has been pointed out that the microstructure of the CP film (PAA in this case) plays a very important role in the dispersion of PtNPs [17], which act as highly active catalysts for the electro-oxidation of H_2O_2. Curve 4b shows how the incorporation of PtNPs on the composite effectively increased its conductivity and catalytic activity. There is a clear synergistic effect between the conducting polymer and the nanoparticle catalyst.

3.4. Effect of scan rate. Optimization of pH and working potentials

Fig. S4 shows the scan rate analysis for the PtNPs/PAA/aSPCEs in 0.1 M PB solution in the presence of 10 mM H_2O_2. The anodic peak currents showed a linear relationship with the square root of the scan rate in the range of 10–400 $mV{\cdot}s^{-1}$ ($R^2 = 0.99714$), indicating that a diffusion controlled electron process occurred for H_2O_2 electrooxidation, which is the ideal situation for quantitative determinations. Moreover, the oxidation potential kept nearly constant at scan rates below 100 mVs^{-1} (see the inset), suggesting a facile charge transfer kinetics over this sweep rate range [37].

The effect of pH on the PtNPs/PAA/aSPCEs was studied from 4.5 to 7.5 in 0.1 M PB by LSV containing 10 mM H_2O_2 (Fig. S5). The optimal response to H_2O_2 appeared at pH 6.5-7.0. Therefore pH 7.0 was chosen for the following experiments for physiological reasons.

The effect of the potential applied on the PtNPs/PAA/aSPCEs is displayed in Fig. S6. The current response was relatively weak at 0.05 V and higher at voltages from 0.1 to 0.3 V. However, the highest potentials are not attractive for practical applications in real samples due to the risk of oxidation of other substances which might cause positive interferences/error during H_2O_2 determinations. Therefore an applied potential of 0.1 V was chosen as the working potential in subsequent experiments.

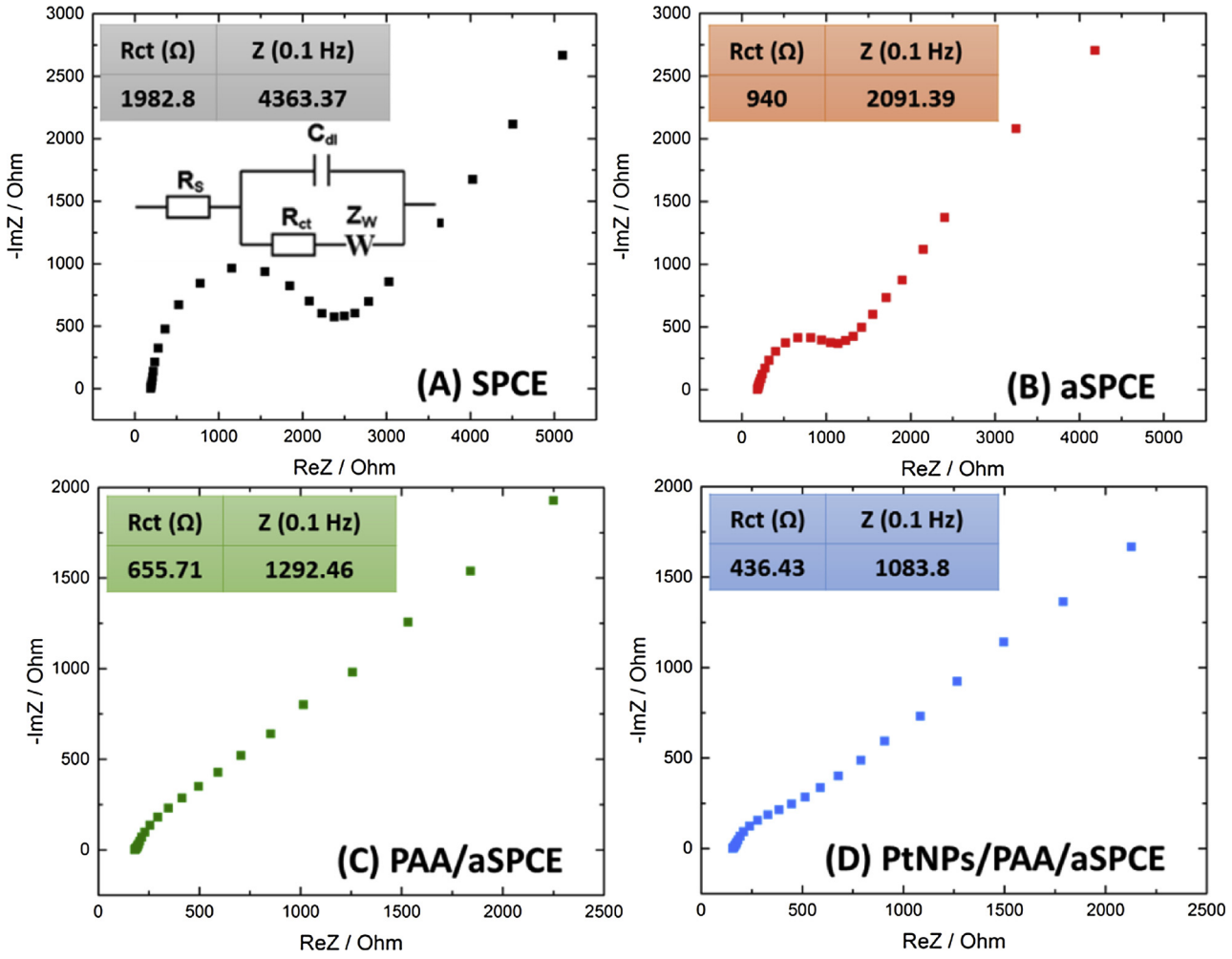

Fig. 2. EIS spectra of the different modified electrodes. The inset in (A) shows the Randles circuit model. The obtained R_{ct} and Z values are displayed in their corresponding spectrum.

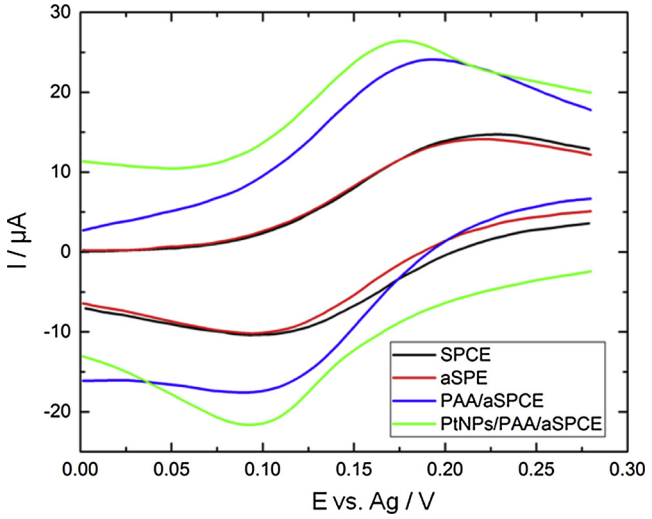

Fig. 3. Zoom of the background-subtracted cyclic voltammograms of the different modified electrodes in 0.1 M KNO_3 containing 5 mM $[Fe(CN)_6]^{4-}$ obtained by subtracting the CVs corresponding to the supporting electrolyte in the absence of $[Fe(CN)_6]^{4-}$.

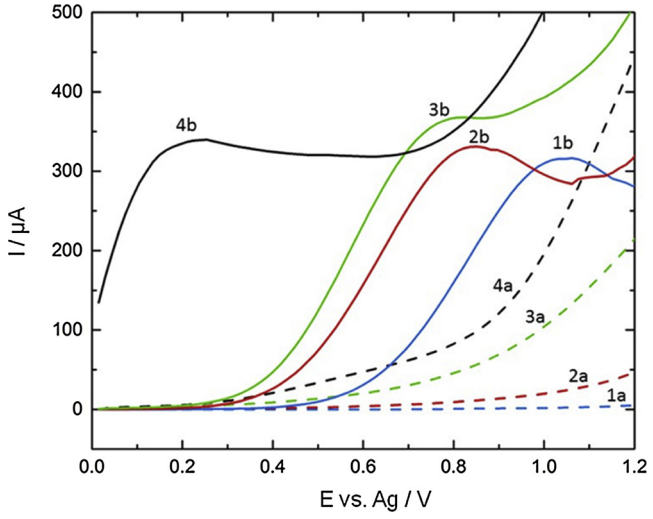

Fig. 4. Anodic LSV responses of the different electrode modification steps in 0.1 M PB in the absence (1a, 2a, 3a and 4a) and presence (1b, 2b, 3b and 4b) of H_2O_2 10 mM. Blue (SPCE), red (aSPCE), green (PAA/aSPCE) and black (PtNPs/PAA/aSPCE) (For interpretation of the references to colour in this figure legend, the reader is referred to the web version of this article).

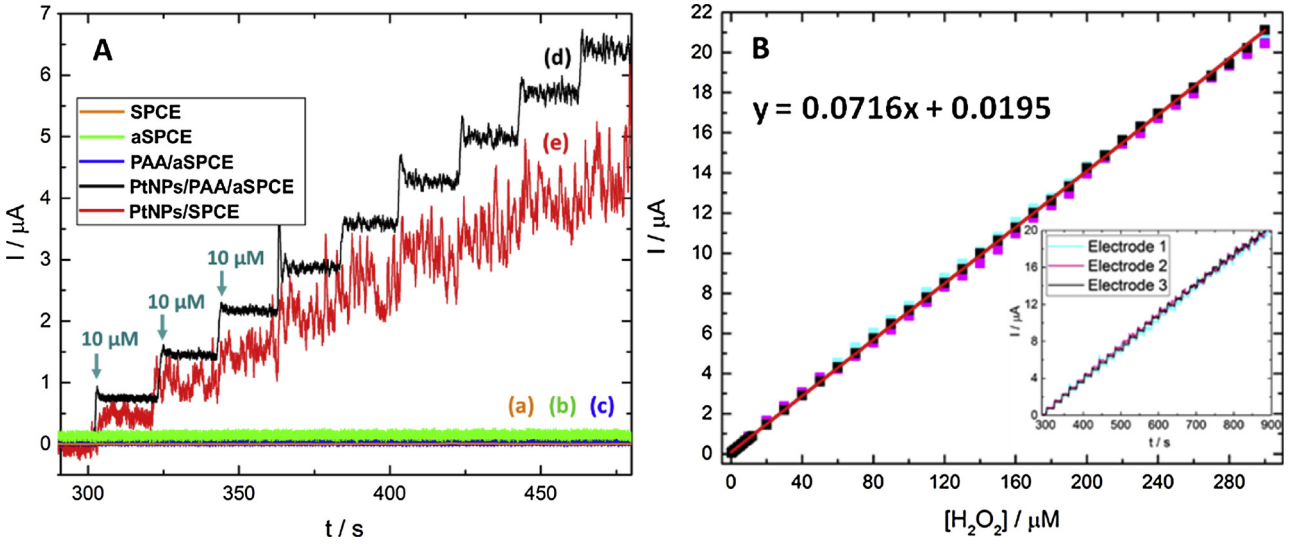

Fig. 5. (A) Amperometric response of the different modified electrodes upon successive additions of 10 µM H_2O_2 in PB (pH 7) at 0.1 V *vs* Ag-SPCE. **(B)** Calibration straight lines obtained from the current increases for three PtNPs/PAA/aSPCEs. The inset shows the amperometric response of three PtNPs/PAA/aSPCEs upon successive additions of 10 µM H_2O_2 in PB at 0.1 V *vs* Ag-SPCE.

3.5. Determination of H_2O_2. Repeatability, reproducibility and stability of the sensor

For comparison, the amperometric responses of the bare SPCE, aSPCEs, PAA/aSPCEs and PtNPs/PAA/aSPCEs to successive additions of H_2O_2 are shown in Fig. 5A. In addition, the response of a bare SPCE modified with PtNPs (curve e), but not including the previous stages of pretreatment of activation and polymerization (PtNPs/SPCE), has also been added to the comparative plot. As seen, SPCE (a), aSPCEs (b) and PAA/aSPCEs (c) did not exhibit any amperometric response to H_2O_2 at 0.1 V. PtNPs/SPCEs (e) exhibited a lower and noisy amperometric response at this low potential. Conversely, PtNPs/PAA/aSPCEs (d) showed a well-defined step response. Increasing the PtNPs loading in the multilayered assembly (data not shown) did not present any improvement in property and the linear range narrowed.

The different electrochemical behavior for PtNPs/SPCEs and PtNPs/PAA/aSPCEs can be explained by the PtNPs dispersion and surface properties. The porous structure derived from the amorphous nature of CPs (PAA) facilitates the dispersion of NPs into the polymer matrix, which increases the specific area of these materials and improves catalytic efficiency [17,38]. Also, due to the high electronic conductivity of the polymer, charge is able to be transmitted along the polymer chains towards the dispersed metals where the electrocatalytic reaction occurs [18]. Another reason that explains the different behavior of these electrodes is the reportedly role of the CP in reducing the poisoning intermediates and improving the catalytic activity of the PtNPs dispersed on polymers [39]. This would explain the lower noise observed for PtNPs/PAA/aSPCEs.

Fig. 5B shows a linear calibration plot exhibiting a good linear response from 0 to 300 µM for three different electrodes. The current generated was used to calculate the sensitivity and limit of detection (LOD) of the system (R^2 = 0.99962), obtaining LOD of 51.6 nM estimated at a S/N ratio of 3, and a sensitivity value of 0.2047 ± 0.0041 µA·µM^{-1} cm^{-2}. The inset shows a continuous amperometry plot at three PtNPs/PAA/aSPCEs electrodes polarized at 0.1 V in response to 10 µM H_2O_2 additions in 0.1 M PB. The net increase in current intensity after each addition was measured and compared with the previous one within this concentration range (see Fig. S7). The catalytic activity remained nearly unchanged during the continuous measurement of H_2O_2 at 10 µM additions from 0 to 300 µM, with a RSD = 4.4%. The measurements carried out with different electrodes, performed on different days, showed the same amperometric response to H_2O_2 concentration. The reproducibility of the analytical response was measured over this range for six PtNPs/PPA/aSPCEs assembled from different preparations, which resulted in a RSD = 2.3%. Regarding the stability of the sensor, we found that this exhibited 100% of the signal after 10 uses and tested on different days (each use means a calibration straight line with 10 consecutive additions of H_2O_2). Moreover, 100% of the signal was also achieved after 1 week when the electrodes were stored under ambient air conditions at room temperature. After this time, a soft electrochemical cleaning by cyclic voltammetry in PB is recommended before use, which can extend the use time at least up to 3 months.

Moreover, it is well known that amperometric assays performed under stirred conditions can be more sensitive than those developed in cyclic voltammetry [40]. Fig. 6 displays the amperometric responses of the PtNPs/PAA/aSPCEs upon successive additions of low concentrations of H_2O_2 in a stirred PB solution. The oxidation current responses of the sensor increased with the successive additions of different concentrations of H_2O_2 in a proportional and homogeneous way, showing excellent reproducibility and high sensitivity, which enables measurements of 200 nM H_2O_2 (Fig. 6B) with a clear and measurable increase in current intensity.

Some significant analytical parameters of the proposed sensor were compared with other modified screen-printed electrodes (SPEs) previously published (Table 2). Sensitivity and LOD value of PtNPs/PAA/aSPCEs in the present study were much better than the values reported in most articles found in the literature. Besides, the working potential applied in this study is lower than some other procedures based on H_2O_2 oxidation. In addition, it can be said that PtNPs/PAA/aSPCEs have also some important advantages such as a simple, reusable, low cost, disposable and easy of modification for the detection of H_2O_2.

3.6. Effect of Interferences

One of the most important challenges of applying amperometric sensors to real samples is to minimize the effect of interfering species. To evaluate the selectivity of the modified electrode, a number of common possible interfering species in the determination of H_2O_2, namely citric acid (CA), glucose, mannitol, salicylic acid (SA), ascorbic acid (AA), dehydroascorbic acid (DHA), urea and resveratrol were investigated on the oxidation peak current of H_2O_2. Fig. 7 shows the amperometric responses of the PtNPs/PAA/aSPCE sensor to the addition of 50 µM H_2O_2 and 50 µM of these species into constantly stirred

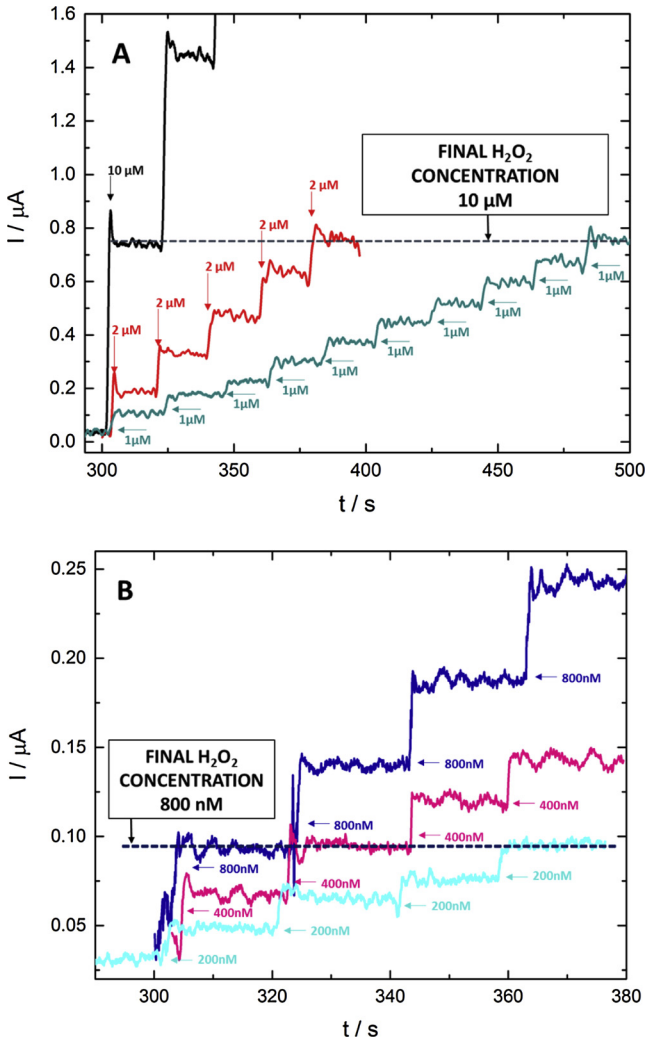

Fig. 6. Amperometric responses of PtNPs/PAA/aSPCEs in 5 mL PB for successive additions of 1, 2 and 10 µM **(A)** and 0.2, 0.4 and 0.8 µM **(B)** of H_2O_2 at 0.1 V *vs* Ag-SPCE.

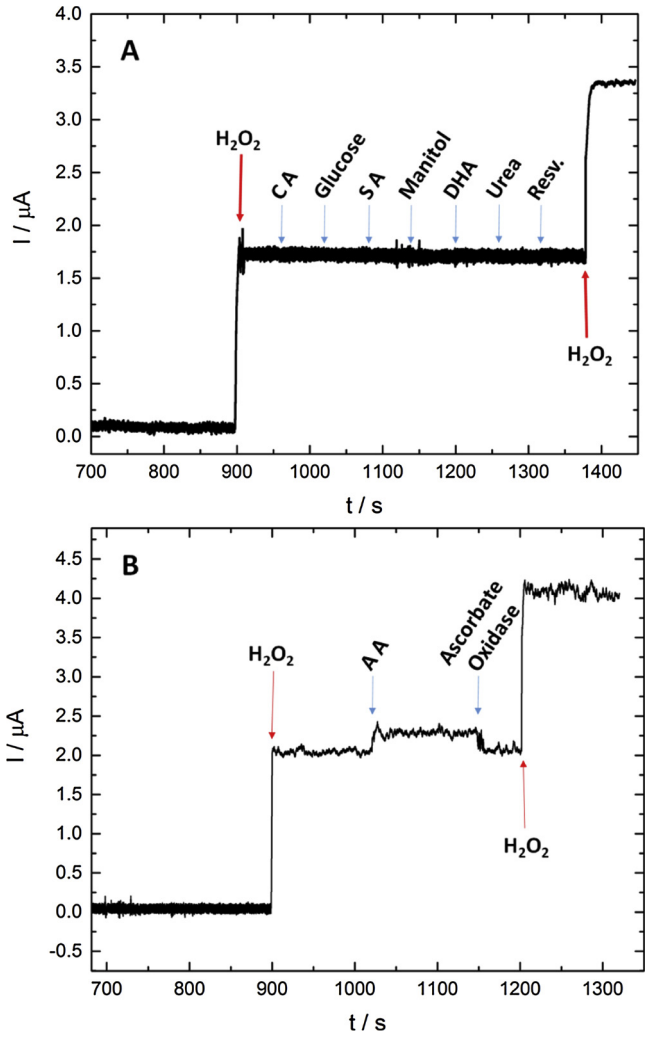

Fig. 7. Amperometric responses of PtNPs/PAA/aSPCE to the successive addition of 50 µM H_2O_2 and 50 µM of the interfering species CA, glucose, SA, mannitol, DHA, urea, resveratrol **(A)**, ascorbic acid and ascorbate oxidase **(B)** in 0.1 M PB at an applied potential of 0.1 V *vs* Ag-SPCE.

Table 2
Comparison of electroanalytical parameters for a variety of modified SPEs.

Electrode [a]	Applied potential (V) (Reference electrode)	LOD (µM)	Reference
PAA(DS)|SPCE	0.5 *vs* Ag	1.4	[22]
Glass/AgNP–PVA	−05, -0.6 *vs* Ag/AgCl	0.30	[41]
PtNP-CNF-PDDA|SPCEs	0.5 *vs* Ag/AgCl	2.4	[42]
PtNPs@SPCEs	0.7 *vs* Ag	1.9	[25]
PtSPE/ZnONPs/GA/GGP	−0.23 *vs* Ag	84	[43]
SPGFE/MWCNTC/PtNP	−0.4 V *vs* Ag/AgCl	1.23	[44]
PtNPs/PAA/aSPCE	0.1 *vs* Ag	0.05	This work

[a] CNF: carbon nanofibers, GA: glutaraldehyde, GGP: guinea grass peroxidase, MWCNTC: multi-walled carbon nanotube clusters, PDDA: poly(diallyldimethylammonium) chloride, PVA: poly(vinyl alcohol), SPGFE: screen-printed gold film electrode.

PB. When some of these species were added to the medium, no current changes were observed in the case of CA, glucose, SA, mannitol, DHA, urea and resveratrol (Fig. 7A). Ascorbic acid was studied separately since it is usually the most problematic interfering compound in the determination of H_2O_2 [45,46]. Fig. 7B shows the amperometric response obtained with the addition of 50 µM H_2O_2 and 50 µM AA. As can be seen, AA only had a small influence on the signal, always below 10% of the signal generated for H_2O_2 at the same concentration. Nevertheless, this interference effect could be easily eliminated by the addition of ascorbate oxidase [47] since the product of the enzymatic catalysis, DHA, does not interfere the signal. Therefore, it can be clearly seen that the prepared electrodes exhibit excellent selectivity for H_2O_2, and that possible interferences caused by AA can be readily eliminated with a previous treatment of the sample with ascorbate oxidase.

3.7. Application to Real Samples

Finally, in order to assess the applicability of the modified electrodes, a series of real samples containing known concentrations of H_2O_2 were analyzed. Selected samples consisted of antiseptic liquids, liquid oxygen bleaching for colored and white clothing, hair lightener and liquid oxygen solution for plants. The peroxide concentration in these samples was also calculated by a conventional spectrophotometric method with xylenol orange (results displayed in Fig. S8 of the Supplementary Material). For the purpose of validating the sensor, three 1:100 dilutions of each real sample were prepared. Then, different volumes of these solutions were added to get a final concentration of 10 µM in all cases. The RSD thus obtained was 2.1%. The results obtained with both methods varied by less than 2% (see Table 3) which highlights the good precision of PtNPs/PAA/aSPCEs for H_2O_2 sensing.

Table 3
H_2O_2 concentration found in different real samples measured by the electrochemical and spectrophotometric techniques.

Real sample	[H_2O_2] M Spectrophotometric Method	[H_2O_2] M Electrochemical Method	Recovery (%)
Antiseptic	0.88 ± 0.37	0.88 ± 0.003	100.0%
Hair lightener	1.02 ± 0.01	1.03 ± 0.009	100.9%
Liquid oxygen solution for plants	2.97 ± 0.05	3.00 ± 0.12	101.0%
Liquid oxygen bleaching for colored clothing	1.45 ± 0.05	1.48 ± 0.19	102.0%
Liquid oxygen bleaching for **white** clothing	1.88 ± 0.05	1.91 ± 0.02	101.5%

4. Conclusions

In summary, an efficient non-enzymatic, disposable, low cost and simple ultrasensitive H_2O_2 sensor based on PtNPs/PAA/aSPCE nanocomposites was prepared by *in situ* growth of well-dispersed Pt nanoparticles on PAA. The assembly of PAA-capped PtNPs built on a previously activated screen printed surface allowed a low coverage of PtNPs, which enhance the electrocatalytic activity towards the oxidation of H_2O_2. The combination of the unique properties of each component endows PtNPs/PAA/aSPCEs as a good electrode material. These novel PtNPs/PAA/aSPCEs hybrids show high sensitivity, stability, repeatability and reproducibility with a detection limit as low as 51.6 nM (S/N = 3) without interference from common electroactive species. In addition, the system was validated by measuring hydrogen peroxide concentrations in different real commercial samples, with similar results to those obtained by a standard spectrophotometric method.

Funding sources

This work was funded by the Spanish Ministry of Economy and Competitiveness (MINECO, http://www.mineco.gob.es/portal/site/mineco/idi), Project No. BFU2016-75609-P (cofunded with FEDER funds, EU), and by the Junta de Comunidades de Castilla-La Mancha (Spain), Project No. SBPLY/17/180501/000276/2 (cofunded with FEDER funds, EU). BGM is a post-doctoral research fellow of the Youth Employment Initiative (JCCM, Spain, cofunded with ESF funds, EU). The funders had no role in study design, data collection and analysis, decision to publish, or preparation of the manuscript.

Declaration of Competing Interest

None.

Acknowledgements

Thanks are given to Dr. Jesús Iniesta from the University of Alicante (Spain) for his helpful with the XPS instrumentation.

Appendix A. Supplementary data

Supplementary material related to this article can be found, in the online version, at doi:https://doi.org/10.1016/j.snb.2019.126878.

References

[1] S. Corveleyn, G.M.R. Vandenbossche, J.P. Remon, Near-infrared (NIR) monitoring of H2O2 vapor concentration during vapor hydrogen peroxide (VHP) sterilisation, Pharm. Res. 14 (1997) 294–298.
[2] Q. Yu, Z. Shi, X. Liu, S. Luo, W. Wei, A nonenzymatic hydrogen peroxide sensor based on chitosan-copper complexes modified multi-wall carbon nanotubes ionic liquid electrode, J. Electroanal. Chem. 655 (2011) 92–95.
[3] M.T. Pérez-Prior, R. Gómez-Bombarelli, M.I. González-Sánchez, E. Valero, Biocatalytic oxidation of phenolic compounds by bovine methemoglobin in the presence of H2O2: quantitative structure-activity relationships, J. Hazard. Mater. 241 (2012) 207–215.
[4] R.C. Matos, E.O. Coelho, C.F. de Souza, F.A. Guedes, M.A.C. Matos, Peroxidase immobilized on amberlite IRA-743 resin for on-line spectrophotometric detection of hydrogen peroxide in rainwater, Talanta 69 (2006) 1208–1214.
[5] K. Żamojć, M. Zdrowowicz, D. Jacewicz, D. Wyrzykowski, L. Chmurzyński, Fluorescent probes used for detection of hydrogen peroxide under biological conditions, Crit. Rev. Anal. Chem. 46 (2016) 171–200.
[6] M.I. González-Sánchez, L. González-Macia, M.T. Pérez-Prior, E. Valero, J. Hancock, A.J. Killard, Electrochemical detection of extracellular hydrogen peroxide in Arabidopsis thaliana: a real-time marker of oxidative stress, Plant Cell Environ. 36 (2013) 869–878.
[7] D. Pan, S. Rong, G. Zhang, Y. Zhang, Q. Zhou, F. Liu, M. Li, D. Chang, H. Pan, Amperometric determination of dopamine using activated screen-printed carbon electrodes, Electrochemistry 83 (2015) 725–729.
[8] S. Chakraborty, C.R. Raj, Pt nanoparticle-based highly sensitive platform for the enzyme-free amperometric sensing of H_2O_2, Biosens. Bioelectron. 24 (2009) 3264–3268.
[9] B.J. Privett, J.H. Shin, M.H. Schoenfisch, Electrochem. Sens. Anal. Chem. 82 (2010) 4723–4741.
[10] S. Palanisamy, S.M. Chen, R. Sarawathi, A novel nonenzymatic hydrogen peroxide sensor based on reduced graphene oxide/ZnO composite modified electrode, Sens. Actuators B Chem. 166 (2012) 372–377.
[11] X. Chen, G. Wu, Z. Cai, M. Oyama, X. Chen, Advances in enzyme-free electrochemical sensors for hydrogen peroxide, glucose, and uric acid, Microchim. Acta 181 (2014) 689–705.
[12] P.T. Lee, L.M. Goncalves, R.G. Compton, Electrochemical determination of free and total glutathione in human saliva samples, Sens. Actuators B Chem. 221 (2015) 962–968.
[13] H. Filik, A.A. Avan, Conducting polymer modified screen-printed carbon electrode coupled with magnetic solid phase microextraction for determination of caffeine, Food Chem. 242 (2018) 301–307.
[14] C. Martin, C. Grgicak, The effect of repeated activation on screen-printed carbon electrode cards, ECS Trans. 61 (2014) 1–8.
[15] M.I. González-Sánchez, B. Gómez-Monedero, J. Agrisuelas, J. Iniesta, E. Valero, Highly activated screen-printed carbon electrodes by electrochemical treatment with hydrogen peroxide, Electrochem. Commun. 91 (2018) 36–40.
[16] A. Ehsani, F. Babaei, M. Nasrollahzadeh, Electrosynthesis and absorbance spectra of TiO2 nanoparticles dispersed in the conductive polymer, Appl. Surf. Sci. 283 (2013) 1060–1064.
[17] D. Zhai, B. Liu, Y. Shi, L. Pan, Y. Wang, W. Li, R. Zhang, G. Yu, Highly sensitive glucose sensor based on pt nanoparticle/polyaniline hydrogel heterostructures, ACS Nano 7 (2013) 3540–3546.
[18] A. Malinauskas, Electrocatalysis at conducting polymers, Synth. Met. 107 (1999) 75–83.
[19] J. Agrisuelas, M.I. González-Sánchez, E. Valero, Electrochemical properties of poly (azure A) films synthesized in sodium dodecyl sulfate solution, J. Electrochem. Soc. 164 (2016) G1–G9.
[20] M.A. Mohamoud, A.R. Hillman, The effect of anion identity on the viscoelastic properties of polyaniline films during electrochemical film deposition and redox cycling, Electrochim. Acta 53 (2007) 1206–1216.
[21] J. Agrisuelas, J.J. García-Jareño, P. Rivas, J.M. Rodríguez-Mellado, F. Vicente, Electrochemistry and electrocatalysis of a Pt@poly(neutral red) hybrid nanocomposite, Electrochim. Acta 171 (2015) 165–175.
[22] J. Agrisuelas, M.I. González-Sánchez, B. Gómez-Monedero, E. Valero, A comparative study of poly(azure A) film-modified disposable electrodes for electrocatalytic oxidation of H_2O_2: effect of doping anion, Polymers 10 (2018) 1–14.
[23] P.H. Deng, Y.L. Feng, J.J. Fei, A new electrochemical method for the determination of trace molybdenum(VI) using carbon paste electrode modified with sodium dodecyl sulfate, J. Electroanal. Chem. 661 (2011) 367–373.
[24] C. Yang, J. Zhao, J. Xu, C. Hu, S. Hu, A highly sensitive electrochemical method for the determination of Sudan I at polyvinylpyrrolidone modified acetylene black paste electrode based on enhancement effect of sodium dodecyl sulphate, Int. J. Environ. Anal. Chem. 89 (2009) 233–244.
[25] J. Agrisuelas, M.I. González-Sánchez, E. Valero, Hydrogen peroxide sensor based on in situ grown Pt nanoparticles from waste screen-printed electrodes, Sens. Actuators B Chem. 249 (2017) 499–505.
[26] R. Jiménez-Pérez, J.M. Sevilla, T. Pineda, M. Blázquez, J. Gonzalez-Rodriguez, Electrocatalytic performance enhanced of the electrooxidation of gamma-hydroxybutyric acid (GHB) and ethanol on platinum nanoparticles surface. A contribution to the analytical determination of GHB in the presence of ethanol, Sens, Actuators B Chem. 256 (2018) 553–563.
[27] D. Ravi Shankaran, N. Uehara, T. Kato, A metal dispersed sol-gel biocomposite amperometric glucose biosensor, Biosens. Bioelectron. 18 (2003) 721–728.
[28] J. Lu, I. Do, L.T. Drzal, R.M. Worden, I. Lee, Nanometal-decorated exfoliated graphite nanoplatelet based glucose biosensors with high sensitivity and fast response, ACS Nano 2 (2008) 1825–1832.

[29] H. Qian, Y. Zhu, R. Jin, Atomically precise gold nanocrystal molecules with surface plasmon resonance, Proc. Natl. Acad. Sci. U. S. A. 109 (2012) 696–700.
[30] R.W. Noble, Q.H. Gibson, The reaction of ferrous horseradish peroxidase with hydrogen peroxide, J. Biol. Chem. 245 (1970) 2409–2413.
[31] C.A. Schneider, W.S. Rasband, K.W. Eliceiri, NIH image to imageJ: 25 years of image analysis, Nat. Methods 9 (2012) 671–675.
[32] S. Trasatti, O.A. Petrii, Real surface area measurements in electrochemistry, J. Electroanal. Chem. 327 (1992) 353–376.
[33] Pierce Biotechnology, Pierce ® quantitative peroxide assay kits, Thermo Sci. 0747 (2012).
[34] P. Chen, R.L. McCreery, Control of electron transfer kinetics at glassy carbon electrodes by specific surface modification, Anal. Chem. 68 (1996) 3958–3965.
[35] R.M. Crooks, M. Zhao, L. Sun, V. Chechik, L.K. Yeung, Dendrimer-encapsulated metal nanoparticles: synthesis, characterization, and applications to catalysis, Acc. Chem. Res. 34 (2001) 181–190.
[36] A. Bard, L. Faulkner, Electrochemical Methods: Fundamentals and Applications, 2nd ed., Wiley, New York, 2001.
[37] M.A. Kamyabi, N. Hajari, Low potential and non-enzymatic hydrogen peroxide sensor based on copper oxide nanoparticle on activated pencil graphite electrode, J. Braz. Chem. Soc. 28 (2017) 808–818.
[38] R.C. Zhang, D. Sun, R. Zhang, W.F. Lin, M. Macias-Montero, J. Patel, S. Askari, C. McDonald, D. Mariotti, P. Maguire, Gold nanoparticle-polymer nanocomposites synthesized by room temperature atmospheric pressure plasma and their potential for fuel cell electrocatalytic application, Sci. Rep. 7 (2017) 46682.
[39] M.G. Abd El-Moghny, H.H. Alalawy, A.M. Mohammad, A.A. Mazhar, M.S. El-Deab, B.E. El-Anadouli, Conducting polymers inducing catalysis: enhanced formic acid electro-oxidation at a Pt/polyaniline nanocatalyst, Int. J. Hydrogen Energy 42 (2017) 11166–11176.
[40] S.A. Kitte, B.D. Assresahegn, T.R. Soreta, Electrochemical determination of hydrogen peroxide at a glassy carbon electrode modified with palladium nanoparticles, J. Serbian Chem. Soc. 78 (2013) 701–711.
[41] A. Ghosale, K. Shrivas, M.K. Deb, V. Ganesan, I. Karbhal, P.K. Bajpai, R. Shankar, A low-cost screen printed glass electrode with silver nano-ink for electrochemical detection of H2O2, Anal. Methods 10 (2018) 3248–3255.
[42] P.J. Lamas-Ardisana, O.A. Loaiza, L. Añorga, E. Jubete, M. Borghei, V. Ruiz, E. Ochoteco, G. Cabañero, H.J. Grande, Disposable amperometric biosensor based on lactate oxidase immobilised on platinum nanoparticle-decorated carbon nanofiber and poly(diallyldimethylammonium chloride) films, Biosens. Bioelectron. 56 (2014) 345–351.
[43] P.A. Uribe, C.C. Ortiz, D.A. Centeno, J.J. Castillo, S.I. Blanco, J.A. Gutiérrez, Self-assembled Pt screen printed electrodes with a novel peroxidase panicum maximum and zinc oxide nanoparticles for H2O2 detection, Colloids Surf. A Physicochem. Eng. Asp. 561 (2019) 18–24.
[44] X. Niu, H. Zhao, C. Chen, M. Lan, Platinum nanoparticle-decorated carbon nanotube clusters on screen-printed gold nanofilm electrode for enhanced electrocatalytic reduction of hydrogen peroxide, Electrochim. Acta 65 (2012) 97–103.
[45] Y. Ni, Y. Liao, M. Zheng, S. Shao, In-situ growth of Co3O4nanoparticles on mesoporous carbon nanofibers: a new nanocomposite for nonenzymatic amperometric sensing of H2O2, Microchim. Acta 184 (2017) 3689–3695.
[46] S. Karakaya, Y. Dilgin, Flow injection amperometric analysis of H2O2 at platinum nanoparticles modified pencil graphite electrode, Electroanalysis 29 (2017) 1626–1634.
[47] M.I. González-Sánchez, J. Agrisuelas, E. Valero, R.G. Compton, Measurement of total antioxidant capacity by electrogenerated iodine at disposable screen printed electrodes, Electroanalysis 29 (2017) 1316–1323.